

FLUID EXCHANGE ACROSS THE EQUATORIAL FRONT*

JIANG Chuan-li (姜传丽), LU Jian (吕建), WU De-xing (吴德星)
(*Institute of Physical Oceanography, Ocean University of Qingdao, Qingdao 266003, China*)

Received Apr. 3, 2000; revision accepted July 7, 2000

Abstract In this paper, the cusp-shaped wave pattern (Legeckis wave) along the Equatorial Front (EF) is modeled by a meandering jet, and the motion of fluid parcels in a two-dimensional kinematic model of the meandering jet along EF is studied using Melnikov's method. Results indicated that the velocity field of the cusp-shaped wave pattern can indeed be modeled by a meandering jet; that the EF will act as a barrier to fluid exchange if there is no variability, but that it is just the variability that moves the buoy across the EF.

Key words: meandering jet, EF, Legeckis wave, Melnikov's method

INTRODUCTION

Legeckis (1977) first reported the appearance of a cusp-shaped wave along the EF (Equatorial Front) in the eastern Pacific in infrared photographs from geostationary weather satellite data. These waves were typically about 1000 km long, extending between about 95°W and 130°W. The waves moved westward at average speed of about 40 cm/s, and effective period of 20 to 30 days. Similar wave patterns had been seen in geostationary satellite data for the summer months of each year since 1975 (Legeckis et al., 1983), except 1976 and 1982, both of which were El Niño years in the eastern tropical Pacific. See Fig. 1.

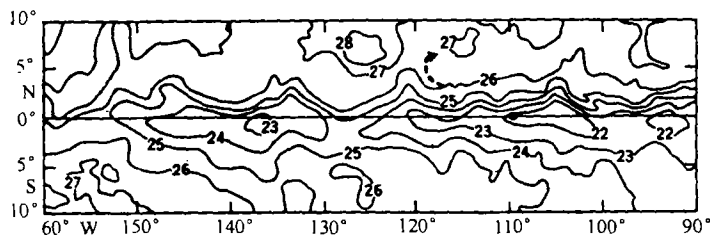


Fig. 1 Sea surface temperature (Philander and Halpern, 1985)

A composite sketch (Fig. 2) shows the Legeckis waves at the equatorial sea surface temperature front (EF) as well as the South Equatorial Current (SEC) and North Equatorial Countercurrent (NECC) (from Legeckis 1977). Philander (1976, 1978) suggested that Legeckis waves result from the shear instability between the SEC and NECC.

Since EF is the equatorial front of sea surface temperature, the fluid around the EF must not be mixed well, otherwise the front will not exist and persist. Then, does the EF really play the role of a barrier for fluid exchange as we intuitively imagined? Fig. 3 shows an exemplary feature in the buoy trajectory (Hansen and Paul, 1984). The buoy was deployed on June 7 (Julian Day 158) at

* Project 49876011 supported by NSFC and Project 98042301 supported by RFDP.

2°N, 105°W. This trajectory also shows a clear example of the buoy behavior in crossing the EF. (position of EF can be seen from Fig. 2)

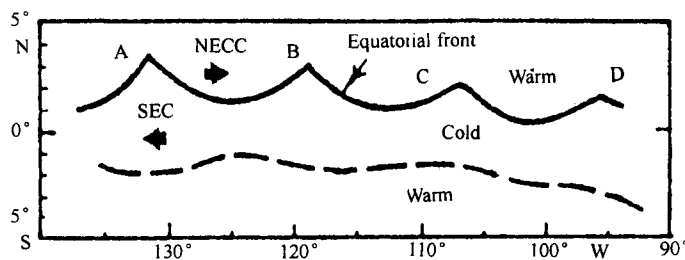


Fig. 2 Sketch of EF, SEC and NECC

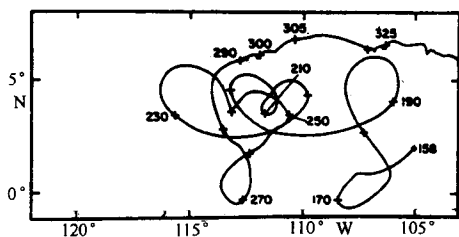


Fig. 3 Trajectory of buoy deployed at 2°N, 105°W (Hansen and Paul, 1984)

Then, the question is how to study the fluid exchange across the EF and how to explain the behavior of the buoy? In this paper, we explain why we can use a meandering jet to model the cusp-shaped wave pattern and to investigate the fluid exchange across the EF by the kinematic model of meandering jet. There were several studies of such Gulf Stream (GS) models in the past few years. Bower (1991), based on RAFOS float observations, devised a kinematic model consisting of a uniform width jet deformed by a steadily propagating sinusoidal meander. In the reference frame

moving with the meander, the fluid motion was steady, the steady motion in the moving frame was comprised of three regimes: a central jet, exterior retrograde motion, and intermediate closed circulation above meander troughs and below crests. But in Bower's model, no exchange can occur between the three regimes.

Samelson (1992) modified Bower's model to include additional spatio-temporal variability in the velocity field to explain the float observations indicating that fluid exchange does occur across some parts of the GS.

CHARACTERISTIC OF VELOCITY FIELD

The cusp-shaped wave pattern along the EF is the shape of isotherms, but what we are concerned about is the characteristic of the velocity field which we now know little about. Here we give a rough but important relation between isotherms and streamlines.

Observations suggest that the cusp-shaped wave pattern can be maintained for several months, so we can conclude that the fluid exchange and mixing must not occur intensely. Based on this conclusion, we suppose isotherms act as barriers to fluid (under ideal condition), i.e. $\frac{d\theta}{dt} = 0$.

Expressing temperature field as $\psi(x, y, t)$, stream function in the fixed frame as $\phi(x, y, t)$, stream function in the reference frame moving with c as $\varphi(x, y, t)$, we get $\varphi = \psi + cy$. Now we are going to obtain the prerequisite of $\frac{\partial \theta}{\partial t} + J(\psi, \theta) = 0$ (1)

Suppose $\xi = x - ct$, we obtain $\frac{\partial \theta}{\partial t} = \frac{\partial \theta}{\partial \xi} \cdot \frac{\partial \xi}{\partial t} = -c \frac{\partial \theta}{\partial \xi}$. From (1), we have

$$-c \frac{\partial \theta}{\partial \xi} + \frac{\partial \psi}{\partial x} \frac{\partial \theta}{\partial y} - \frac{\partial \psi}{\partial y} \frac{\partial \theta}{\partial x} = 0$$

$$-c \frac{\partial \theta}{\partial \xi} + \frac{\partial \psi}{\partial \xi} \frac{\partial \theta}{\partial y} - \frac{\partial \psi}{\partial y} \frac{\partial \theta}{\partial \xi} = 0$$

$$\frac{\partial \psi}{\partial \xi} \frac{\partial \theta}{\partial y} + [-c - \frac{\partial \psi}{\partial y}] \frac{\partial \theta}{\partial \xi} = 0$$

Letting $\varphi = \psi + cy$, we get $\frac{\partial \varphi}{\partial \xi} = \frac{\partial \psi}{\partial \xi}$, $\frac{\partial \varphi}{\partial y} = \frac{\partial \psi}{\partial y} + c$. Substituting this formula into the former formula, we have

$$\frac{\partial \varphi}{\partial \xi} \frac{\partial \theta}{\partial y} - \frac{\partial \varphi}{\partial y} \frac{\partial \theta}{\partial \xi} = 0, J(\varphi, \theta) = 0 \Leftrightarrow \theta = F(\varphi) \quad (2)$$

It easily follows that $\theta = F(\varphi)$ is the sufficient condition of (1):

$$\theta = F(\varphi) \Rightarrow J(\varphi, \theta) = 0 \Rightarrow \frac{\partial \varphi}{\partial x} \frac{\partial \theta}{\partial y} - \frac{\partial \varphi}{\partial y} \frac{\partial \theta}{\partial x} = 0 \xrightarrow{\xi=x-ct} \frac{\partial \varphi}{\partial \xi} \frac{\partial \theta}{\partial y} - \frac{\partial \varphi}{\partial y} \frac{\partial \theta}{\partial \xi} = 0$$

$$\xrightarrow{\varphi=\psi+cy} \frac{\partial \psi}{\partial \xi} \frac{\partial \theta}{\partial y} + [-c - \frac{\partial \psi}{\partial y}] \frac{\partial \theta}{\partial \xi} = 0 \Rightarrow -c \frac{\partial \theta}{\partial \xi} + \frac{\partial \psi}{\partial \xi} \frac{\partial \theta}{\partial y} - \frac{\partial \psi}{\partial y} \frac{\partial \theta}{\partial \xi} = 0$$

$$\Rightarrow \frac{\partial \theta}{\partial \xi} \frac{\partial \xi}{\partial t} + \frac{\partial \psi}{\partial x} \frac{\partial \theta}{\partial y} - \frac{\partial \psi}{\partial y} \frac{\partial \theta}{\partial x} = 0 \Rightarrow \frac{\partial \theta}{\partial t} + \frac{\partial \psi}{\partial x} \frac{\partial \theta}{\partial y} - \frac{\partial \psi}{\partial y} \frac{\partial \theta}{\partial x} = 0 \Rightarrow \frac{\partial \theta}{\partial t} + J(\psi, \theta) = 0$$

From the above conditions, the existence of EF requires that the temperature field and the velocity field satisfy the condition that the isotherms and the streamlines are parallel. Observations showed that the EF indeed exists, so the streamlines must parallel the isotherms. We should note here that our premise that fluid exchange and mixing across the EF does not exist; but this is not in fact the case, so our conclusion that streamlines are parallel to the isotherms is correct only on an ideal condition. While we here consider the streamlines "basically" parallel to the isotherms, they will be affected by other fluctuations which will be discussed later.

MODEL

So the stream function for the cusp-shaped wave pattern along the EF can be taken to have the form studied by Bower (1991) and Samelson (1992) for the GS:

$$\psi^* = \psi_0 \left\{ \tanh\left(\frac{y^* - y_c^*}{\lambda^* / \cos \alpha^*}\right) - 1 \right\} \quad (3)$$

where

ψ_0 : scale factor, which with λ^* , determines the maximum downstream speed;

$$y_c^*: A^* \cos[k^*(x^* - c^*t^*)] + \frac{1}{2} k^* d^{*2} \cos[2k^*(x^* - c^*t^*)] +$$

$$\frac{3}{8} k^{*2} d^{*3} \cos[3k^*(x^* - c^*t^*)]$$

define the center streamline, where A^* is wave amplitude, the last two terms correct the shape of streamline to make it more similar to the cusp-shaped wave pattern; $k^* = \frac{2\pi}{L^*}$, the wave number;

λ^* : the scale width of the jet; $\alpha^* = \tanh\left(\frac{\partial y_c^*}{\partial x}\right)$, direction of current;

A reference frame moving with the meander may be introduced with coordinates:

$$\xi = x - ct \quad (\text{in this paper, } c \text{ is negative}), \eta = y$$

The corresponding non-dimensional stream function for motion in the co-moving frame is:

$$\varphi(\xi, \eta) = \tanh\left(\frac{\eta - \eta_c}{\cos^{-1} \alpha}\right) - 1 + c\eta \tag{4}$$

where

$$\varphi(\xi, \eta) = \psi(\xi, \eta) + c\eta$$

$$\eta_c = B \cos(k\xi) + \frac{1}{2} k d^2 \cos(2k\xi) + \frac{3}{8} k^2 \delta^3 \cos(3k\xi);$$

$$\alpha = \tan^{-1}\left(\frac{\partial \eta_c}{\partial \xi}\right)$$

Based on our observation of the Legeckis wave, we will fix the parameters for the basic meandering jet at the following values (Table 1):

Table 1 Parameter values for basic meandering jet

Dimensional	Non-dimensional
$\lambda^* = 100 \text{ km}$	$\lambda = 1$
$L^* = 1000 \text{ km}$	$L = 10$
$k^* = \frac{2\pi}{L^*} = \frac{2\pi}{1000 \text{ km}}$	$k = \frac{2\pi}{10}$
$A^* = 100 \text{ km}$	$B = 0.5$
$C_r^* = -40 \text{ cm/s}$	$c = -1/3$
$d^* = 50 \text{ km}$	$\delta = 0.5$

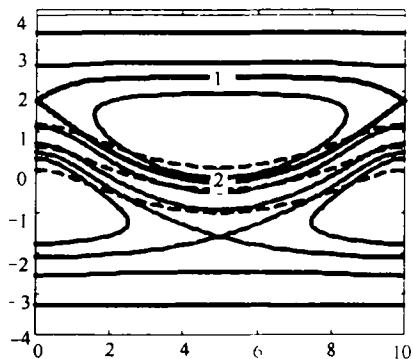


Fig.4 Contours of stream-function

Results are shown in Fig.4:

Dotted lines are the contours of the stream-function in the fixed frame (x, y) at $t = 0$, solid lines are the contours of the stream-function in the co-moving frame. In fact, these contours correspond to streamlines in the co-moving frame and completely describe the flow, because φ is time independent. The velocity field in the moving frame can be divided into three distinct types (as mentioned in Introduction) by two boundary streamlines labeled 1 and 2, through which no fluid will cross, so that no transport of fluid parcels into or out of the jet can occur in the moving frame.

Now we consider three different types of variability: a time-dependent, spatially uniform meridional velocity; a time-dependent meander amplitude; and a propagating plane wave superimposed on the basic flow (1).

Melnikov's method

These variabilities may cause boundary 1 and 2 to break so that fluid exchange may occur. Melnikov's method is a rigorous technique for calculating (to first order) the instantaneous local distance between these boundaries. This distance is a measure of the gap through which exchange occurs.

The expression for the Melnikov's distance d is:

$$d = \epsilon d_M(t_0) = \frac{\epsilon M(t_0)}{|U[X^0(0)]|}$$

where $M(t_0)$ is the Melnikov function, which provides a compact estimate of the amount of exchange between three regimes (see Samelson, 1992 for details).

RESULTS

Spatially uniform meridional flow

Seawater along the equator flows polarward under the effect of Ekman pumping. This meridional velocity has seasonal period, and can be expressed as follows:

$$v = \cos(\omega t + \delta)$$

Substitution of this variability into (4) yields the total velocity as:

$$\begin{aligned} \dot{\xi} &= -\frac{\partial \varphi}{\partial \eta} \\ \dot{\eta} &= \frac{\partial \varphi}{\partial \xi} + \varepsilon \cos(\omega t + \delta) \end{aligned}$$

which is Melnikov function as expressed below:

$$\begin{aligned} M(t_0) &= \int_{-\infty}^{+\infty} \{U[X^0(t)]v'[X^0(t), t + t_0] + V[X^0(t)]u'[X^0(t), t + t_0]\} dt \\ &= \int_{-\infty}^{+\infty} U[X^0(t)]\cos(\omega t + \delta) dt \end{aligned} \quad (5)$$

$$M(t_0) = \int_{-\infty}^{+\infty} U[X^0(t)][\cos(\omega t)\cos(\omega t_0 + \delta) - \sin(\omega t)\sin(\omega t_0 + \delta)] dt$$

$$\text{Suppose } \int_{-\infty}^{+\infty} U[X^0(t)]\cos(\omega t) dt = M_1; \int_{-\infty}^{+\infty} U[X^0(t)]\sin(\omega t) dt = M_2$$

So, we get

$$M(t_0) = M_1 \cos(\omega t_0 + \delta) - M_2 \sin(\omega t_0 + \delta)$$

$$\text{Let } M_0 = \sqrt{M_1^2 + M_2^2}, \quad M(t_0) = \sqrt{M_1^2 + M_2^2} \cos(\omega t_0 + \delta')$$

$$\text{then} \quad M(t_0) = M_0 \cos(\omega t_0 + \delta') \quad (6)$$

For both boundary 1 and 2, the Melnikov function is the cosine of t_0 , and $M(t_0)$ have finite discrete null points, which means instantaneous boundary lines coincide. The instantaneous boundary lines 1 and 2 coincide or separate in time, so fluid exchange may occur. The amount of fluid exchange depends on the value of amplitude M_0 .

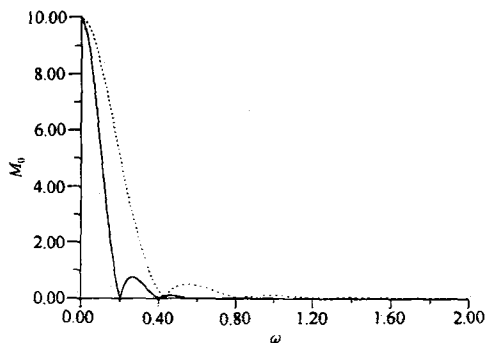


Fig.5 Amplitude M_0 of the Melnikov function with frequency $\tilde{\omega}$ for meridional flow

Since M_0 cannot be expressed theoretically, we calculate M_0 numerically for boundary 1 and 2. Results are shown in Fig.5.

In Fig.5, the solid line is for boundary 1, and dotted line for boundary 2. When $\omega = 0$, both M_0 reach maximal value 10, which coincide well with the theoretical result of (6). It suggests that constant meridional velocity variability can make fluid exchange larger than the time-dependent variability; in addition, within the limits of $\omega(0 - 0.4)$, the strength of the fluid exchange through boundary 2 is larger than that through boundary 1. That means that the amount of exchange between recirculation and the retrograde

regimes is larger and that the fluid exchange across boundary 2 is easier.

Fluctuating meander amplitude

Following Samelson (1992), we allow the meander amplitude to vary in time by letting B have the following form:

$$B = B_0 + \epsilon \cos(\omega t + \delta)$$

Substituting this expression into (5) and Taylor expansion in ϵ gives:

$$\varphi(\xi, \eta, B) = \varphi(\xi, \eta, B_0) + \epsilon \varphi' + o(\epsilon^2)$$

where $\varphi' = \frac{\partial \varphi(\xi, \eta, B_0)}{\partial B} \cos(\omega t + \delta)$.

For this stream-function the Melnikov function is:

$$M(t_0) = \int_{-\infty}^{+\infty} \{ u[X^0(t)] \cdot v'[X^0(t), t + t_0] - v[X^0(t)] \cdot u'[X^0(t), t + t_0] \} dt$$

we can easily reduce the above formula to:

$$M(t_0) = M_0 \cos(\omega t_0 + \delta') \tag{7}$$

The results are shown in Fig.6. Again, solid line for boundary 1 and dotted line for boundary 2:

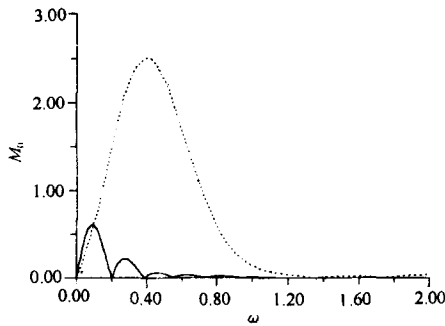


Fig.6 Similar to Fig.5, except for fluctuating meander amplitude

The most striking feature of Fig.6 is that the maximum exchange and the frequency range over which significant exchange occurs for boundary 2 are larger than those for boundary 1.

Propagating plane waves

The meandering jet along the EF will be affected by equatorial waves, so we consider zonal propagating plane waves variability having the following form:

$$\varphi'(\xi, \eta, t) = k_p^{-1} \cos[k_p(\xi - C_p \cdot t) + \delta] \tag{8}$$

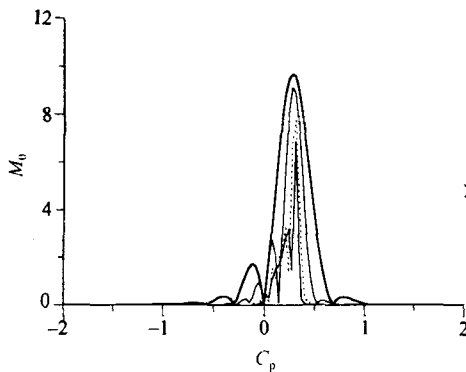


Fig.7 $M_0(C_p)$ for boundary 1

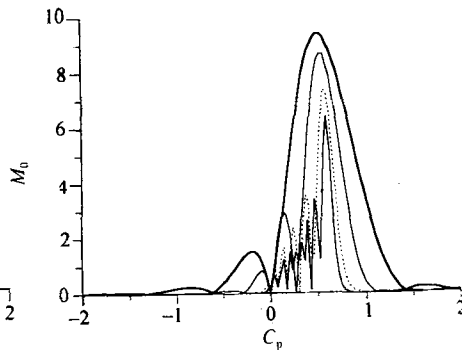


Fig.8 $M_0(C_p)$ for boundary 2

The Melnikov function of (8) has the same form as (7). The results $M_0(C_p)$ are shown in Fig. 7 and Fig. 8 (for boundary 1 and 2 respectively). The thinner solid line, dotted line, solid line, thicker solid line are for four different plane wave wavelengths $2\pi/C_p$: 10, 5, 2, 1. As the wavelength increases, the frequency range over which significant exchange occurs are larger, that is to say, long plane waves (their phase speeds match the basic flow velocity) can facilitate strong fluid exchange.

From the above calculations, we can conclude that these three types of variability can indeed induce strong fluid exchange. This gives full proof for the buoy trajectories crossing the cusp-shaped wave pattern.

SUMMMARY

In this work, fluid exchange across the EF was studied by using a kinematic model of a meandering jet and the method of Melnikov. Results indicated that for certain meridional velocity fluctuation and meander amplitudes variability, the strength of fluid exchange depends strongly on the frequency of the variability, some certain frequency can cause strong fluid exchange. While propagating plane waves can cause stronger exchange with increasing wavelength, the exchange is very strong when phase speed matches the basic flow velocities. So we can say that it is variability that determines the buoy trajectory mentioned above.

We must note here that this model involves only kinematics, and does not consider any dynamical factor. But we have seen that this model can help us understand the fluid exchange across the EF and know more about the buoy behavior.

References

- Bower, A. S., 1991. A simple kinematic mechanism for mixing fluid parcels across a meandering jet. *J. Phys. Oceanogr.* **21**: 173 - 180.
- Hansen, D., Paul, C., 1984. Genesis and effects of long waves in the equatorial Pacific. *J. Geophys. Res.* **89**: 10431 - 10440.
- Legeckis, R., 1977. Long waves in the eastern equatorial Pacific Ocean: A view from a geostationary satellite. *Science* **197**: 1197 - 1181.
- Legeckis, R., Pichel, W., Nesterczuk, G., 1983. Equatorial long waves in geostationary satellite observations and in a multichannel sea surface temperature analysis. *Bulletin American Meteorological Society* **64**(2): 133 - 139.
- Philander, G., Halpern, D., 1985. Long waves in the equatorial Pacific Ocean. *Eos* **66**(14): 1 - 154.
- Philander, S. G. H., 1976. Instabilities of zonal equatorial current. *J. Geophys. Res.* **81**(21): 3725 - 3735.
- Philander, S. G. H., 1978. Instabilities of zonal equatorial current, 2. *J. Geophys. Res.* **83**(C7): 3679 - 3682.
- Samelson, R. M., 1992. Fluid exchange across a meandering jet. *J. Phys. Oceanogr.* **22**: 431 - 440.